

Synthesis and characterization of pectin & xanthan / zinc oxide biopolymer-based functional films for food packaging

Sheetal D. Deshmukh^{1*}, Fasaha Ahmad¹, Vijay B. Pawade² & Sushil U. Lokhande¹

¹Department of Food Technology, Laxminarayan Innovation Technological University, Nagpur – 440 033, Maharashtra, India

²Department of Physics, Laxminarayan Innovation Technological University, Nagpur – 440 033, Maharashtra, India

*E-mail: sheetaldeherajdeshmukh11@gmail.com

Received 23 January 2026; accepted 9 April 2026

With increasing demand for sustainable and eco-friendly alternatives to conventional plastic packaging, this work focuses on the development of biodegradable films derived from natural biopolymers. In this study, a composite film was formulated using xanthan gum and pectin in a 2:1 ratio (xanthan gum:pectin), selected based on their compatibility and ability to form mechanically strong and flexible matrices. Four film formulations — XG-P-ZO, XG-P-C, XG-P-ZO-C, and XG-P (control) — were developed through solution casting followed by drying at ambient conditions, and further analysed by physicochemical, mechanical, and functional tests to determine their suitability for food packaging applications. Moisture content, water vapour permeability, water absorption, and tensile strength were examined under standard test conditions. Among the formulations, XG-P-C exhibited the highest tensile strength (1.366 MPa compared to 0.647 MPa for the control), while XG-P-ZO showed the lowest moisture content (5.02%). Water solubility was lowest in XG-P-C (34.56% vs. 57.50% for the control). Antioxidant activity was measured by DPPH scavenging, which exhibited the best performance in the combined additive film, found to be 89.54%, with incorporation of curcumin and zinc oxide. XRD, SEM, and FTIR analysis were also carried out to determine the nature of the film, surface morphology, and presence of functional groups in the formulated films. However, water vapour permeability results indicated that additive incorporation did not improve vapour barrier performance compared to the control, suggesting the need for further matrix optimization. Thus, from the present investigation, the xanthan gum–pectin composite films with zinc oxide and curcumin exhibited improved mechanical strength, antioxidant activity, and controlled moisture absorption while maintaining biodegradability, and show considerable promise as sustainable active packaging materials for extending food shelf life and reducing environmental impact.

Keywords: Antioxidant, Biodegradable films, Biopolymer, Food Packaging, Xanthan gum–pectin composite

Introduction

The increasing reliance on synthetic plastics in the food packaging industry has raised serious environmental concerns due to their non-biodegradability and accumulation in landfills and natural ecosystems. Conventional plastics, while inexpensive and durable, degrade extremely slowly, contributing to long-term environmental pollution and posing threats to marine life, soil health, and overall ecosystem balance¹. In response, there has been a growing shift in research and industrial practices towards sustainable alternatives, particularly biodegradable packaging materials derived from natural sources. Among these, biopolymer-based films have emerged as promising candidates, offering an eco-friendlier solution without significantly compromising the functional requirements of packaging^{2,3}.

Biopolymers are naturally occurring polymers obtained from renewable resources such as plants, animals, algae, and microorganisms⁴. Common

examples include starch, cellulose, gelatine, chitosan, agar, alginate, xanthan gum, and pectin. These materials are favoured for their biodegradability, edibility, non-toxicity, and ability to form continuous films when cast from solution⁵. However, despite these advantages, biopolymer-based films often exhibit poor mechanical strength, high water sensitivity, and low barrier properties compared to synthetic plastics⁶. To address these shortcomings, recent research has focused on polymer blending and the incorporation of functional additives such as nanoparticles and antioxidants to enhance the physical, structural, and functional properties of biodegradable films^{6,7}.

Among the available polysaccharide-based biopolymers, xanthan gum and pectin have shown significant potential in food packaging applications. Xanthan gum is an anionic extracellular polysaccharide produced by the bacterium *Xanthomonas campestris*. It is widely used in the food and pharmaceutical industries due to its high viscosity, thermal stability, and film-

forming ability⁸. However, films prepared solely from xanthan gum tend to be brittle and prone to moisture absorption. Pectin, another natural polysaccharide primarily derived from citrus peels and apple pomace, is known for its excellent gelling properties and capacity to form flexible films^{8,9}. When used in combination, xanthan gum and pectin can exhibit synergistic effects, improving film strength, integrity, and barrier properties due to enhanced intermolecular interactions.

The strategy of blending xanthan gum and pectin can lead to the formation of a compatible biopolymeric matrix that combines the favourable properties of both polymers. Xanthan gum imparts viscosity and thickening capability, while pectin contributes to flexibility and structural integrity⁹. The choice of a 2:1 ratio of xanthan gum to pectin in this study was based on preliminary tests that showed this combination provided optimal mechanical strength and flexibility for film formation. This ratio ensures a balanced interaction between the highly branched xanthan gum molecules and the linear chains of pectin, resulting in a stable matrix suitable for food packaging applications¹⁰.

To further enhance the functional performance of these biopolymer films, the incorporation of active agents such as zinc oxide (ZnO) and curcumin has been explored. ZnO is a widely studied inorganic compound known for its antimicrobial, UV-blocking, and barrier-enhancing properties¹¹. When added to biopolymer films, ZnO nanoparticles can significantly improve tensile strength, reduce water vapour permeability, and extend the shelf life of packaged food by inhibiting microbial growth. The mechanism of reinforcement involves hydrogen bonding and physical interactions between the ZnO particles and the polymer chains, which enhance film compactness and structural rigidity¹².

Curcumin, a polyphenolic compound extracted from the rhizome of *Curcuma longa* (turmeric), is well-known for its potent antioxidant, antimicrobial, anti-inflammatory, and colouring properties. It has gained popularity as a natural additive in food packaging materials due to its ability to scavenge free radicals and prevent oxidative spoilage of food products¹³. Additionally, curcumin imparts a natural yellowish hue to the film, contributing both aesthetic and functional value. When incorporated into biopolymer films, curcumin can enhance antioxidant capacity, reduce oxidative degradation, and offer a form of active packaging that contributes to food preservation¹⁴⁻¹⁷.

The antioxidant mechanisms of ZnO and curcumin are complementary. ZnO nanoparticles can donate electrons to neutralize free radicals through surface redox reactions, addressing radical chain initiation, while curcumin acts primarily through hydrogen atom transfer (HAT) and single electron transfer (SET) mechanisms to interrupt radical propagation. Together, these dual mechanisms may provide superior antioxidant protection compared to either additive alone. Furthermore, curcumin's phenolic hydroxyl groups may interact with surface hydroxyl groups on ZnO particles, enhancing dispersion within the polymer matrix and improving interfacial compatibility¹⁴.

This study focuses on the development of biodegradable films using a blend of xanthan gum and pectin, with the incorporation of zinc oxide and curcumin as reinforcing and functional agents, respectively. Four film formulations were developed for comparative analysis: a control film containing only the xanthan gum–pectin blend; a film with zinc oxide; a film with curcumin; and a composite film containing both zinc oxide and curcumin. These films were fabricated using the solvent casting method and subjected to various physicochemical, mechanical, and morphological tests to evaluate their potential for use in food packaging.

Several studies have examined pectin-xanthan blends³ and ZnO incorporation in biopolymer films^{12,15} individually. However, a comprehensive comparison of ZnO and curcumin, both alone and in combination, within a xanthan gum–pectin matrix with simultaneous evaluation of mechanical, barrier, antioxidant, and biodegradability properties represents the novel contribution of the present work. The use of curcumin in colloidal dots form as a dispersible functional agent also distinguishes this study from prior reports using bulk curcumin powder¹⁶.

The specific objectives of this study were: (1) to develop xanthan gum–pectin composite films by solution casting; (2) to incorporate ZnO and curcumin as functional additives and compare four formulations; (3) to comprehensively characterize the films by XRD, SEM, FTIR, and physicochemical/mechanical testing; and (4) to evaluate the antioxidant activity and biodegradability of the developed films for food packaging applications.

Experimental Section

Chemicals

During preliminary screening trials, several biopolymers were tested for their film-forming ability

and mechanical performance, including chitosan, agar, pectin, cellulose, xanthan gum, and gelatine. Based on the mechanical integrity and visual quality of the resulting films, xanthan gum and pectin were selected for the final formulation development. All chemicals including xanthan gum, pectin, glycerol, zinc oxide, and curcumin dots solution were sourced from the Food Technology Department Laboratory, Laxminarayan Innovation Technological University, Nagpur. All chemicals were of analytical grade.

Film formation

Based on preliminary optimization, a blend of xanthan gum and pectin in a 2:1 ratio (xanthan gum:pectin) was selected as the most promising combination for film formation. Four distinct film formulations were prepared: XG-P-ZO, XG-P-C, XG-P-ZO-C, and XG-P.

For all formulations, 4 g of xanthan gum was dissolved in 300 mL of distilled water (1.33% w/v), and 2 g of pectin was dissolved in 100 mL of distilled water (2% w/v). These two solutions were mixed thoroughly to ensure complete homogenization. To each mixture, 1 mL of glycerol (0.33% v/v) was added as a plasticizer to enhance film flexibility. The blend was then heated at $70^{\circ}\text{C} \pm 2^{\circ}\text{C}$ with continuous stirring at 300 rpm for 3 h to achieve complete hydration and gelatinization of the biopolymer blend. After gelatinization, the prepared solution was poured into Petri dishes and dried at room temperature for 48 h.

The four formulations differed as follows:

XG-P-ZO Film: This formulation included 0.05 g of zinc oxide (0.05% w/v), added to the pectin–xanthan gum blend to improve the mechanical properties and barrier functions of the film. This concentration was selected based on the lower range reported in similar biopolymer-ZnO composite studies^{12,15}.

XG-P-C Film: In this formulation, 2 to 3 drops of curcumin dots solution (equivalent to approximately 0.1% v/v, consistent with concentrations reported in similar active packaging studies¹⁶) were added to the pectin–xanthan gum blend to provide a natural colour and antioxidant function.

XG-P-ZO-C Film: This formulation combined both zinc oxide (0.05% w/v) and curcumin dots solution (2–3 drops) with the pectin–xanthan gum blend, providing both reinforcement and antioxidant functionality.

XG-P Film: The XG-P film served as the control, containing only the pectin–xanthan gum blend with glycerol, without any additional agents.

Characterization

X-ray Diffraction (XRD)

X-ray diffraction analysis was carried out using a Rigaku Miniflex diffractometer (CuK α radiation, $\lambda = 1.5406 \text{ \AA}$), operated at 40 kV and 15 mA, with a 2θ scanning range of $5\text{--}80^{\circ}$, step size of 0.02° (2θ), and scan speed of $2^{\circ}/\text{min}$. Cooling water flow was maintained at 4.3 L/min.

Scanning Electron Microscopy (SEM)

The surface morphology of the developed films was analysed using Scanning Electron Microscopy (SEM) to assess the impact of zinc oxide and curcumin incorporation.

Fourier Transform Infrared (FTIR) Spectroscopy

FTIR spectroscopy was used to determine the bonding information of the film materials. A Bruker Alpha II FTIR instrument with a diamond crystal ATR accessory was used to record spectra. Vibrational spectra were acquired in the range of $400\text{--}4000 \text{ cm}^{-1}$.

Thickness

Film thickness was measured using an Electronic Thickness Gauge (resolution: 0.01 mm). All thickness measurements were carried out at approximately 18 different points per film, and the corresponding mean values were used in WVP and tensile strength calculations. Three thickness measurements were taken on each tensile testing sample along the strip length.

Tensile Strength (TS) and Elongation at Break (EAB)

Film strips ($100 \text{ mm} \times 10 \text{ mm}$) were tested using a Universal Testing Machine (UTM). Tensile strength was calculated as:

$$\text{TS} = P / (b \times d) \quad \dots (1)$$

Where TS is in MPa; P is the fracture load (N); b is the film width (mm); d is the film thickness (mm).

Moisture content

Moisture content was determined by drying film samples at 105°C in an oven. The formula used was:

$$\text{MC} (\%) = [(m_1 - m_2) / m_1] \times 100 \quad \dots (2)$$

Where m_1 and m_2 are the initial and final (dried) masses, respectively.

Water Solubility

Film strips were dried at $105 \pm 1^{\circ}\text{C}$ for 24 h, then immersed in 50 mL of distilled water at 25°C for 24 h

with periodic stirring. Remaining films were filtered through Whatman No. 1 filter paper and dried again at 105°C for 24 h. Water solubility was calculated as:

$$\text{WS (\%)} = [(\text{initial dry weight} - \text{final dry weight}) / \text{initial dry weight}] \times 100 \quad \dots (3)$$

Water Vapour Permeability (WVP)

The WVP of films was measured gravimetrically using a modified ASTM E96 procedure. Calcium chloride was placed in a beaker to generate 0% RH; the beaker was then sealed with the test film, an O-ring, and vacuum grease to ensure an airtight seal. The beaker was placed inside a desiccator containing silica gel to provide 75% RH. Weight changes (to the nearest 0.0001 g) were recorded over 4 days at room conditions. WVP was calculated as follows.

$$\text{WVP} = (\Delta m \times x) / (t \times A \times \Delta P) \quad \dots (4)$$

Where, WVP is in g/(m·s·Pa); Δm is the mass of moisture permeated through the film; x is the film thickness; t is the measurement time; A is the film area; ΔP is the water vapour pressure difference across the film. Note: this formula calculates WVP (thickness-normalized), not WVTR (area-based). Thickness normalization allows meaningful comparison between films of different thickness.

Water absorption

Water absorption was measured per ASTM D570. Film strips were dried at 105°C for 24 h, then immersed in 50 mL distilled water. Weight gain was recorded at 5, 10, 15, 30, 60, 90, and 120 min intervals. Water absorption was calculated as:

$$\text{WA (\%)} = [(W_{\text{time}} - W_{\text{dry}}) / W_{\text{dry}}] \times 100 \quad \dots (5)$$

Antioxidant activity (DPPH Method)

Antioxidant activity was evaluated using the DPPH radical scavenging assay. About 50 mg of film sample was added to 5 mL DPPH solution (0.004% in methanol) and incubated at room temperature for 30 and 60 min. Absorbance was measured at 517 nm. The ABTS assay was also initially conducted but excluded from final analysis due to unreliable results. The ABTS radical cation (ABTS•+) appeared to be affected by the zinc oxide component, likely through oxidative interference that inflated absorbance readings, resulting in physically meaningless negative scavenging values (-10.17%) for the XG-P-ZO-C film. This assay interference is consistent with known

pro-oxidant behaviour of metal oxides in radical cation-based assays under certain conditions. Therefore, conclusions regarding antioxidant activity are based solely on DPPH results.

$$\text{Free radical scavenging activity (\%)} = [(A_0 - A_s) / A_0] \times 100 \quad \dots (6)$$

Where A_0 and A_s are the absorbances of the DPPH control and test film, respectively.

Biodegradability test

Film specimens of known initial weight (W_i) were buried in natural soil at approximately 5 cm depth and maintained under ambient laboratory conditions for 21 days, with the soil kept slightly moist throughout. After the incubation period, samples were carefully removed, washed with distilled water, and air-dried. The extent of degradation was calculated as follows.

$$\text{Weight loss (\%)} = [(W_i - W_f) / W_i] \times 100 \quad \dots (7)$$

Where W_i is the initial weight of the film before burial and W_f is the final dry weight after excavation, washing, and air-drying.

Statistical analysis

All experiments were conducted in triplicate ($n = 3$). Results are expressed as mean \pm standard deviation (SD). Differences between formulations were assessed qualitatively based on the magnitude of means and standard deviations. Formal statistical significance testing was done using one-way ANOVA with Tukey's post-hoc test.

Results and Discussion

XRD analysis

The XRD patterns of the four film formulations (XG-P, XG-P-ZO, XG-P-C, and XG-P-ZO-C) are shown in Fig. 1. All samples showed a broad diffraction peak centred around $2\theta \approx 20^\circ$, indicating the predominantly amorphous nature of the biopolymer-based films.

XG-P (Control): This film displayed the highest intensity peak, suggesting relatively higher ordered molecular arrangements among the xanthan gum and pectin chains. The broader peak confirms the dominantly amorphous character, but the sharpness implies better packing and less disruption in the polymer matrix.

XG-P-ZO (zinc oxide): The incorporation of zinc oxide led to a reduction in peak intensity compared to

the control, indicating a disruption in the crystallinity of the matrix. This could be due to zinc oxide particles interfering with polymer chain packing, thereby increasing amorphousness. No distinct ZnO crystalline peaks were observed, likely due to its low concentration or good dispersion within the matrix.

XG-P-C (curcumin): This film showed a further decrease in intensity, suggesting that curcumin interfered with the intermolecular interactions between biopolymers, enhancing the disordered structure. Curcumin, being a bulky molecule, may hinder tight packing of polymer chains.

XG-P-ZO-C (zinc oxide + curcumin): The film with both additives exhibited the lowest intensity, indicating the most disordered and amorphous structure among all formulations. This reduced crystallinity is consistent with the lower tensile strength observed for XG-P-ZO-C (0.574 MPa), as reduced molecular order weakens the intermolecular cohesion of the polymer network. The amorphous structure may also account for the higher WVP observed in additive-containing films, as amorphous regions are more permeable to water vapour than crystalline domains.

Overall, the addition of ZnO and curcumin progressively reduced crystallinity, with the most pronounced effect observed in the combined film (XG-

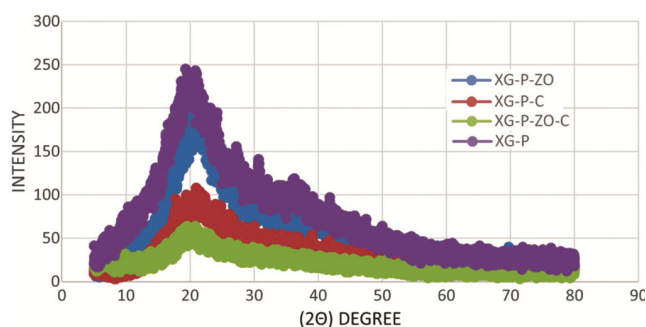


Fig.1 — Comparative XRD patterns of all four films

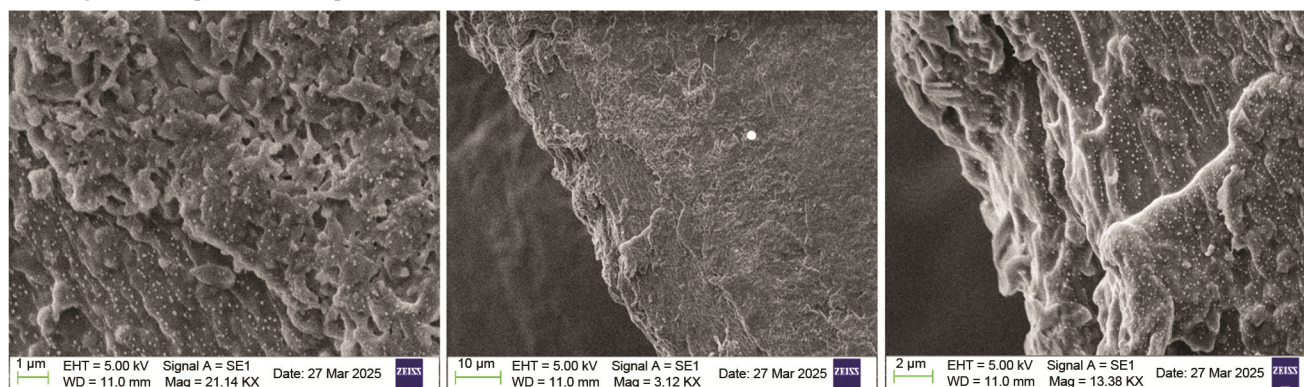


Fig. 2 — SEM images of XG-P-ZO

P-ZO-C). These structural changes directly correlate with the mechanical and barrier property trends discussed in subsequent sections, supporting the conclusion that crystallinity is a key structural determinant of film performance in this biopolymer system.

SEM analysis

SEM analysis provided direct visualization of the surface morphology of the films (Figs 2–5). XG-P-ZO film showed a relatively smooth surface with visible white regions, indicating successful dispersion of zinc oxide particles within the matrix (Fig. 2). XG-P-C film demonstrated a comparatively uniform and flat surface, suggesting good compatibility and dispersion of curcumin dots (Fig. 3). In the XG-P-ZO-C film, the surface exhibited granular structures, likely due to the combined presence of zinc oxide and curcumin, which may have led to partial aggregation and uneven distribution (Fig. 4). This granular morphology is consistent with the reduced tensile strength of XG-P-ZO-C, as particle aggregation can create stress concentration points within the film matrix. In contrast, the control film (XG-P) without additives displayed an irregular and rough morphology, indicating weaker film structure and lower uniformity in the absence of reinforcing components (Fig. 5). The progression from smoother (XG-P-ZO) to rougher (XG-P-ZO-C) surfaces correlates well with the tensile strength data, supporting the hypothesis that filler dispersion quality is a key determinant of mechanical performance in these films.

FTIR analysis

XG-P-ZO

Fig. 6a shows the FTIR spectrum of the XG-P-ZO film. A broad peak around 3300 cm^{-1} is due to O–H

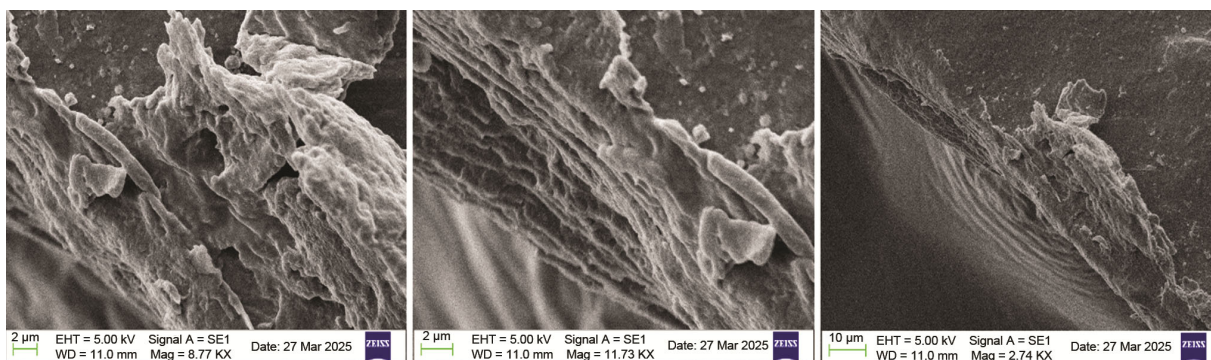


Fig. 3 — SEM images of XG-P-C

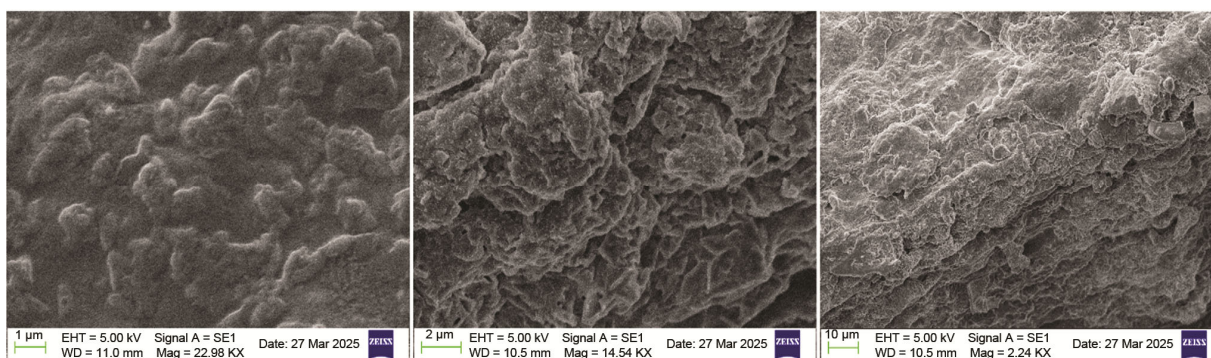


Fig. 4 — SEM images of XG-P-ZO-C

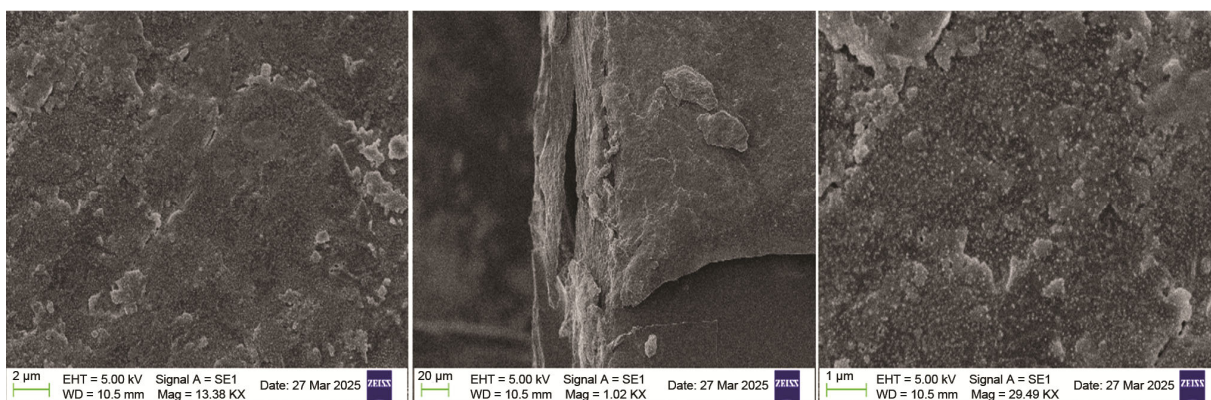


Fig. 5 — SEM images of XG-P

stretching from hydroxyl groups in xanthan gum, pectin, and glycerol. A peak near 2920 cm^{-1} indicates C–H stretching. A small peak around 1720 cm^{-1} corresponds to C=O stretching from ester groups in pectin. The peak near 1600 cm^{-1} is due to COO⁻ stretching from carboxylic groups in the polysaccharides. Peaks in the range of $1000\text{--}1100\text{ cm}^{-1}$ are from C–O and C–O–C bonds typical of sugar-based structures. Peaks below 600 cm^{-1} confirm the presence of Zn–O bonds, indicating successful

incorporation of zinc oxide into the film. The Zn–O absorption band in this range is consistent with the characteristic ZnO vibrational signature reported for ZnO-based pigments by Pawade *et al.*²⁰, further validating the presence and structural integrity of the ZnO phase within the biopolymer matrix. The FTIR-confirmed presence of ZnO is consistent with its role in reducing moisture content (5.02%), as ZnO particles create physical barrier domains that limit water uptake.

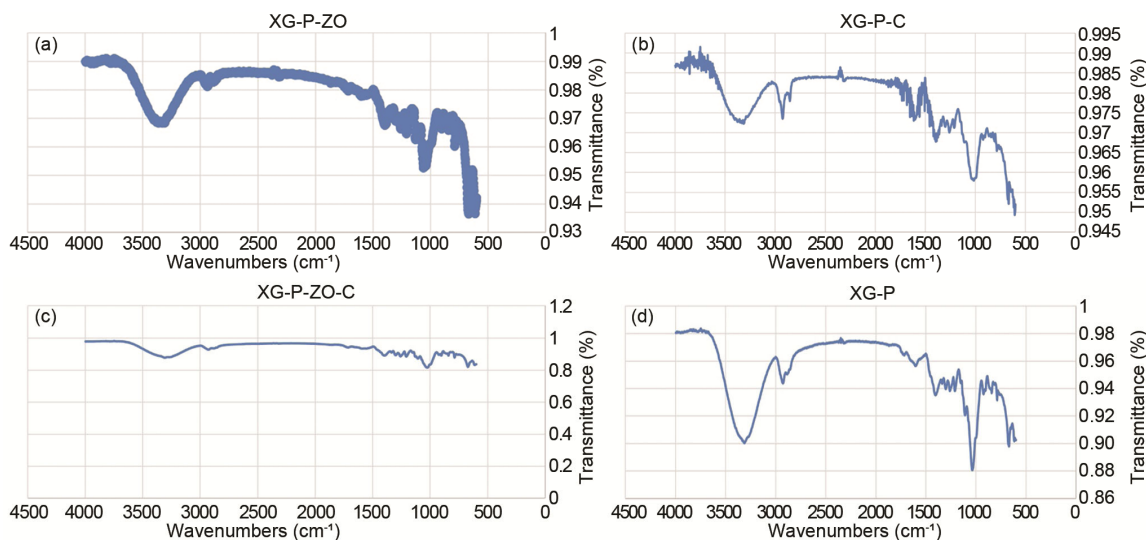


Fig. 6 — FTIR spectra of (a) XG-P-ZO, (b) XG-P-C, (c) XG-P-ZO-C and (d) XG-P films

XG-P-C

The FTIR spectrum of XG-P-C (Fig. 6b) shows a broad peak around 3300 cm^{-1} indicating O–H stretching from polysaccharides and glycerol. The peak at $\sim 2900\text{ cm}^{-1}$ corresponds to C–H stretching. A peak near 1720 cm^{-1} is attributed to C=O stretching from pectin and curcumin. The region around 1600 cm^{-1} indicates C=C stretching from curcumin or $-\text{COO}^-$ groups. Peaks between $1000\text{--}1150\text{ cm}^{-1}$ correspond to C–O–C and C–O bonds from polysaccharides. A small peak around 850 cm^{-1} may represent aromatic bending from curcumin. These peaks confirm the presence and interactions of all film components. The uniform SEM morphology of XG-P-C, combined with the FTIR evidence of curcumin incorporation, is consistent with its highest tensile strength (1.366 MPa), suggesting good polymer-curcumin interfacial compatibility.

XG-P-ZO-C

The FTIR spectrum of XG-P-ZO-C (Fig. 6c) exhibits a broad absorption band around $3300\text{--}3400\text{ cm}^{-1}$ associated with O–H stretching from polysaccharides, glycerol, and curcumin. Peaks near 2915 cm^{-1} are due to C–H stretching. The strong peak around $1730\text{--}1740\text{ cm}^{-1}$ corresponds to C=O stretching from ester or carboxylic acid groups (pectin and curcumin). Peaks at $1600\text{--}1640\text{ cm}^{-1}$ indicate C=C stretching or COO^- groups. Bands between $1000\text{--}1150\text{ cm}^{-1}$ correspond to polysaccharide C–O and C–O–C stretching. A peak in the range of $500\text{--}650\text{ cm}^{-1}$ confirms Zn–O bonding, indicating successful incorporation of zinc oxide nanoparticles.

XG-P

The FTIR spectrum of XG-P (Fig. 6d) exhibits characteristic peaks for xanthan gum, pectin, and glycerol. A broad absorption band around $3280\text{--}3400\text{ cm}^{-1}$ corresponds to O–H stretching and hydrogen bonding. The peak near 2920 cm^{-1} is attributed to C–H stretching. A peak around $1720\text{--}1740\text{ cm}^{-1}$ corresponds to C=O stretching from ester or carboxylic groups in pectin. Peaks at $1600\text{--}1650\text{ cm}^{-1}$ correspond to asymmetric COO^- stretching. Bands at $1000\text{--}1150\text{ cm}^{-1}$ are due to C–O and C–O–C stretching of polysaccharides. The overall spectrum confirms successful blending of biopolymers and plasticizer.

Physicochemical, mechanical, and functional properties of pectin-xanthan composite films

Table 1 summarizes the thickness, moisture content, water solubility, and mechanical properties.

Thickness

The measured mean thicknesses were: XG-P-ZO ($0.281 \pm 0.09\text{ mm}$), XG-P-C ($0.429 \pm 0.23\text{ mm}$), XG-P-ZO-C ($0.239 \pm 0.10\text{ mm}$), and XG-P ($0.358 \pm 0.09\text{ mm}$) (Table 1).

Moisture content

The film containing zinc oxide alone (XG-P-ZO) showed the lowest moisture content at $5.02 \pm 0.25\%$, indicating that zinc oxide contributes to a more compact or less hydrophilic matrix. The control film (XG-P) showed the highest moisture content at $8.05 \pm 0.09\%$, followed by XG-P-ZO-C at $8.00 \pm 0.4\%$ and XG-P-C at $7.22 \pm 0.36\%$. These results (Table 1) suggest that zinc oxide alone is more

Table 1 — Physicochemical, Mechanical, and Functional Properties of Pectin-Xanthan Composite Films

Film Formulation	Thickness (mm)	Moisture content (%)	Water solubility (%)	Tensile strength (MPa)	Elongation at break (mm)	WVP (10^{-10} g/m \cdot s \cdot Pa)	Water absorption (%) (at 120 min)	DPPH scavenging activity (%)
XG-P (Control)	0.358 \pm 0.09	8.05 \pm 0.09	57.50 \pm 2.8	0.647 \pm 0.03	9.9 \pm 0.5	0.72 \pm 0.04	2744.91 \pm 137.2	74.8 \pm 4.3
XG-P-ZO	0.281 \pm 0.09	5.02 \pm 0.25	61.93 \pm 3.1	0.869 \pm 0.04	5.9 \pm 0.3	9.28 \pm 0.04	2472.66 \pm 123.6	84.0 \pm 1.2
XG-P-C	0.429 \pm 0.23	7.22 \pm 0.36	34.56 \pm 1.7	1.366 \pm 0.07	9.27 \pm 0.4	3.03 \pm 0.15	815.13 \pm 40.8	73.5 \pm 2.5
XG-P-ZO-C	0.239 \pm 0.10	8.00 \pm 0.40	56.52 \pm 2.8	0.574 \pm 0.03	14.2 \pm 0.7	5.50 \pm 0.28	875.90 \pm 43.8	89.5 \pm 0.0

effective in reducing moisture absorption than curcumin or their combination. The FTIR-confirmed ZnO incorporation in the XG-P-ZO film supports this interpretation, as ZnO particles create physical barrier domains that limit moisture uptake.

Water solubility

Among the four formulations, the film containing curcumin alone (XG-P-C) showed the lowest water solubility (34.56 \pm 1.7%), suggesting that curcumin reduces the hydrophilicity of the film matrix, possibly through hydrophobic interactions or by partially occupying sites available for water sorption (Table 1). The control film (XG-P) exhibited a water solubility of 57.50 \pm 2.8%. The film with zinc oxide alone (XG-P-ZO) had the highest solubility (61.93 \pm 3.1%), possibly due to the disruption of polymer chain packing by ZnO particles increasing accessible surface area. The dual-additive film (XG-P-ZO-C) showed intermediate behaviour (56.52 \pm 2.8%), suggesting a partial counterbalancing of the ZnO and curcumin effects

Tensile strength and elongation at break

The tensile strength of films was measured to assess mechanical performance (Table 1). Among the formulations, XG-P-C (curcumin only) exhibited the highest tensile strength (1.366 \pm 0.07 MPa), suggesting that curcumin positively influenced structural integrity, possibly by enhancing polymer interactions or film uniformity. XG-P-ZO showed moderate tensile strength (0.869 \pm 0.04 MPa). However, XG-P-ZO-C (both additives) displayed the lowest tensile strength (0.574 \pm 0.03 MPa). This reduction may be attributed to the disruption of the polymer network caused by the combined presence of ZnO particles and curcumin, leading to poor mechanical cohesion. The reduced crystallinity confirmed by XRD for this formulation supports this interpretation. The control film XG-P had a tensile strength of 0.647 MPa.

These results indicate that the choice of formulation should be application-dependent. For mechanically demanding packaging applications, XG-P-C is the preferred formulation. For applications requiring high antioxidant activity (e.g., packaging of fatty foods or fresh produce prone to oxidative spoilage), XG-P-ZO-C offers superior radical scavenging capacity despite of its reduced tensile strength. The importance of rheological and mechanical optimization in biopolymer-based coating systems has also been underscored by Chanpurkar *et al.*²¹, whose work on lactide-based polyester coatings highlights that controlled formulation parameters are essential to achieving consistent mechanical performance.

The elongation at break (EAB) values followed a trend inverse to tensile strength: XG-P-ZO-C exhibited the highest EAB (14.2 \pm 0.7 mm), followed by XG-P (9.9 \pm 0.4 mm), XG-P-C (9.27 \pm 0.4 mm), and XG-P-ZO (5.9 \pm 0.3 mm). The high EAB of XG-P-ZO-C, despite its lowest tensile strength, is consistent with its highly amorphous XRD profile, where reduced molecular order allows greater chain mobility and deformation before rupture. Conversely, ZnO acting as a rigid filler in XG-P-ZO restricted chain mobility, yielding the lowest EAB, while curcumin in XG-P-C enhanced network cohesion at the cost of flexibility — a classic stiffness–ductility trade-off observed in reinforced biopolymer films^{3,16}. The XG-P-ZO-C formulation is therefore more suited for flexible wrap applications, while XG-P-C is preferable where mechanical robustness is the primary requirement.

Water Vapour Permeability (WVP)

The WVP values obtained were: XG-P-ZO: 9.28 \times 10⁻¹⁰ g/(m \cdot s \cdot Pa); XG-P-C: 3.025 \times 10⁻¹⁰ g/(m \cdot s \cdot Pa); XG-P-ZO-C: 5.50 \times 10⁻¹⁰ g/(m \cdot s \cdot Pa); XG-P (control): 7.24 \times 10⁻¹¹ g/(m \cdot s \cdot Pa). Notably, the control film showed the lowest WVP value, while all additive-containing films showed higher WVP. This is interpreted as follows: the incorporation of ZnO and

curcumin disrupted the compact hydrogen-bonded network of the xanthan-pectin matrix (as confirmed by reduced crystallinity in XRD), creating micro-channels that facilitated water vapour transport. This finding indicates that additive incorporation, at the concentrations used, did not improve water vapour barrier performance. Future studies should explore cross-linking strategies or higher ZnO concentrations to achieve improved vapour barrier properties.

Water absorption

All films showed high water absorption, characteristic of uncross-linked polysaccharide-based films. The high percentage values (>800% at 120 min for most films) are calculated on a dry-weight basis using ASTM D570 [$WA\% = (W_{wet} - W_{dry})/W_{dry} \times 100$] and have been re-verified against original laboratory records. For the control film XG-P after 120 min: $W_{dry} = 1.0626$ g, $W_{wet} = 30.2300$ g, giving $WA = [(30.2300 - 1.0626)/1.0626] \times 100 = 2744.91\%$. Such high values for uncross-linked hydrophilic polysaccharide films are consistent with published literature^{3,15}, where pure xanthan films have been reported to absorb over 1000% water by mass.

The XG-P control film exhibited the highest water absorption (2744.91% at 120 min), indicating its high hydrophilicity. XG-P-ZO showed the lowest absorption among films (2472.66%), likely due to its denser matrix. XG-P-C and XG-P-ZO-C showed significantly lower absorption (815.13% and 875.90% respectively), suggesting that curcumin, even at low concentrations, contributes to water resistance. Overall, these results reinforce the need for cross-linking or coating strategies to reduce the high hydrophilicity of these biopolymer films for practical food packaging applications.

Antioxidant activity

The antioxidant activity of the biopolymer films, evaluated by DPPH free radical scavenging, is presented in Table 1. XG-P-ZO-C showed the highest scavenging activity at 89.54%, followed by XG-P-ZO at 84%, XG-P at 74.77%, and XG-P-C at 73.54%.

The higher DPPH scavenging activity of XG-P-ZO (84%) compared to XG-P-C (73.54%) was an unexpected result, as curcumin is widely recognized as a potent antioxidant. This finding may be explained by: (1) the well-documented electron-donation capacity of ZnO nanoparticles, which can donate electrons from their surface to neutralize free radicals through redox mechanisms^{18,19}; and (2) the limited

effective concentration of curcumin used in this study (2–3 drops of colloidal solution), which likely provided a lower molar concentration of active curcumin than the 0.05% w/v ZnO. The superior performance of XG-P-ZO-C (89.54%) suggests that the two additives work through complementary mechanisms — ZnO through electron donation and curcumin through HAT and SET — providing synergistic antioxidant protection. This result is competitive with literature-reported values of 85% DPPH activity for CMC films incorporating both ZnO and curcumin by Roy and Rhim¹⁴.

Biodegradability

The film samples were buried in natural soil for 21 days. Upon excavation, all film formulations had significantly disintegrated and integrated into the soil matrix, with only faint white residues remaining that could not be separated for weighing (Fig. 7). This observation indicates extensive degradation, where the material underwent microbial and environmental breakdown to the point of losing structural integrity. While quantitative weight loss data could not be

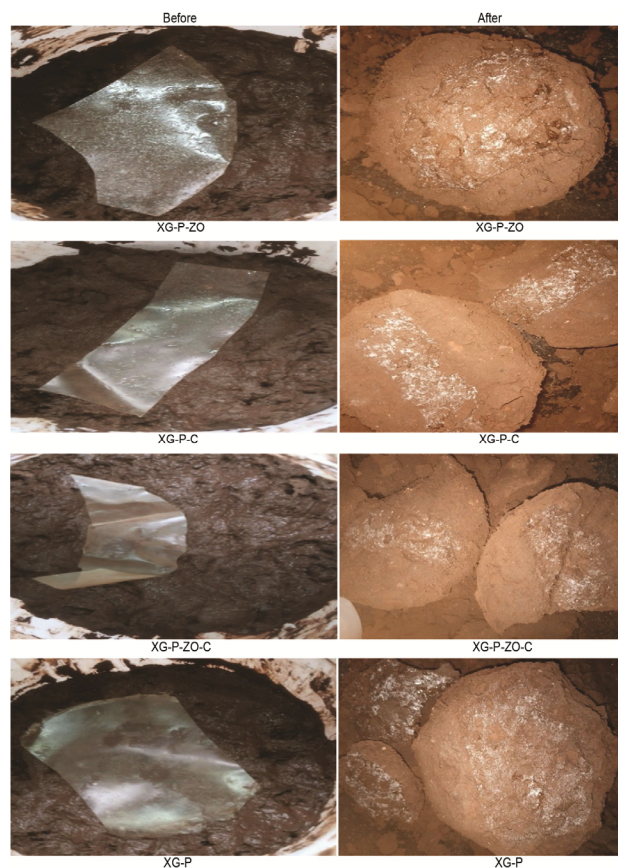


Fig. 7 — Biodegradability test of films with soil (before and after)

obtained due to complete disintegration within 21 days, this qualitative observation confirms effective biodegradability. The rapid degradation is consistent with the hydrophilic, polysaccharide-based nature of the films, which are highly susceptible to microbial attack. Future studies should employ progressive time points (7, 14, 21 days) to capture quantitative weight loss data before complete disintegration occurs.

Conclusion

This study demonstrates the successful development and characterization of biodegradable films from a xanthan gum and pectin blend (2:1 ratio, xanthan gum:pectin) with functional additives zinc oxide and curcumin for food packaging applications. FTIR analysis confirmed the interaction between biopolymers and additives without significant chemical degradation. XRD patterns revealed the semi-crystalline to amorphous nature of the films, with zinc oxide and curcumin reducing crystallinity in a manner that correlated with changes in mechanical and barrier properties. SEM images showed well-dispersed zinc oxide particles contributing to a smoother film surface in XG-P-ZO, while curcumin produced a uniform surface in XG-P-C consistent with its superior tensile strength. Mechanically, XG-P-C exhibited the best tensile strength (1.366 MPa, vs. 0.647 MPa for the control), while XG-P-ZO-C showed the lowest tensile strength (0.574 MPa), indicating that the combined use of ZnO and curcumin disrupts matrix cohesion and requires further optimization. XG-P-ZO demonstrated the most effective moisture reduction (5.02% moisture content), while XG-P-C showed the best water resistance (34.56% solubility). Antioxidant activity was highest in XG-P-ZO-C (89.54% DPPH), demonstrating synergistic action of ZnO and curcumin. However, several important limitations must be acknowledged: (1) the combined XG-P-ZO-C film exhibited the lowest tensile strength, limiting its suitability for applications requiring mechanical robustness; (2) all films showed high water absorption (>800% after 120 min), restricting applicability in high-humidity environments without additional cross-linking; (3) WVP results showed that additive incorporation increased rather than decreased water vapour permeability compared to the control, indicating that the matrix disruption outweighed the potential barrier contribution of ZnO at the concentrations used.

Future work should explore: (a) optimization of ZnO and curcumin concentrations; (b) physical or chemical cross-linking of the biopolymer matrix to improve water resistance and tensile properties; (c) ultrasonication for improved nanoparticle dispersion; (d) antimicrobial testing against relevant food pathogens; (e) real-food shelf-life trials; and (f) formal statistical analysis (ANOVA with Tukey's post-hoc test) with adequate replication. Despite these limitations, the xanthan gum–pectin composite films with zinc oxide and curcumin show application-dependent promise as sustainable active packaging materials capable of contributing to food preservation and reduced environmental impact.

Conflict of Interest

The authors declare no conflict of interest.

References

- 1 Ahmad M M, Chauhan K, Naz A & Nayeem M, Antimicrobial and antioxidant activity of impregnated pectin and alginate based bio composite packaging material for fresh produce safety, *Pharma Innov*, 10 (2021) 262.
- 2 Atef M, Rezaei M & Behrooz R, Preparation and characterization agar-based nanocomposite film reinforced by nanocrystalline cellulose, *Int J Biol Macromol*, 70 (2014) 537.
- 3 Bhatia S, Al-Harrasi A, Shah Y A, Alrasbi A N S, Jawad M, Koca E, Aydemir L Y, Alamoudi J A, Almoshari Y & Mohan S, Structural, mechanical, barrier and antioxidant properties of pectin and xanthan gum edible films loaded with grapefruit essential oil, *Heliyon*, 10 (2024) e25501.
- 4 de Moraes L M, Carneiro L C, Bianchini D, Dias A R G, da Rosa Z E, Prentice C & da Silveira M A, Structural, thermal, physical, mechanical, and barrier properties of chitosan films with the addition of xanthan gum, *J Food Sci*, 82 (2017) 698.
- 5 El-Miri N, Abdelouahdi K, Barakat A, Zahouily M, Fihri A, Solhy A & El-Achaby M, Bio-nanocomposite films reinforced with cellulose nanocrystals, *Carbohydr Polym*, 129 (2015) 156.
- 6 Ge L, Li X, Zhang R, Yang T, Ye X, Li D & Mu C, Development and characterization of dialdehyde xanthan gum crosslinked gelatin based edible films, *Food Hydrocoll*, 51 (2015) 129.
- 7 Jovanović J, Ćirković J, Radojković A, Mutavdžić D, Tanasijević G, Joksimović K, Bakić G, Branković G & Branković Z, Chitosan and pectin-based films and coatings with active components for application in antimicrobial food packaging, *Prog Org Coat*, 158 (2021) 106349.
- 8 Kasirga Y, Oral A & Caner C, Preparation and characterization of chitosan/montmorillonite-K10 nanocomposites films for food packaging applications, *Polym Compos*, 33 (2012) 1874.
- 9 Khoshgozaran-Abras S, Azizi M H, Hamidy Z & Bagheripoor-Fallah N, Mechanical, physicochemical and color properties of chitosan based-films as a function of Aloe vera gel incorporation, *Carbohydr Polym*, 87 (2012) 2058.

- 10 Letendre M, D'Aprano G, Lacroix M, Salmieri S & St-Gelais D, Physicochemical properties and bacterial resistance of biodegradable milk protein films containing agar and pectin, *J Agric Food Chem*, 50 (2002) 6017.
- 11 Li Y, Hu Z, Huo R & Cui Z, Preparation of an indicator film based on pectin, sodium alginate, and xanthan gum containing blueberry anthocyanin extract, *Heliyon*, 9 (2023) e14421.
- 12 Meydanju N, Pirsa S & Farzi J, Biodegradable film based on lemon peel powder containing xanthan gum and TiO₂-Ag nanoparticles, *Polym Test*, 106 (2022) 107445.
- 13 Moraes I C F, Carvalho R A, Bittante A M Q B, Solorza-Feria J & Sobral P J A, Film forming solutions based on gelatin and poly(vinyl alcohol) blends, *J Food Eng*, 95 (2009) 588.
- 14 Roy S & Rhim J W, Carboxymethyl cellulose-based antioxidant and antimicrobial active packaging film incorporated with curcumin and zinc oxide, *Int J Biol Macromol*, 148 (2020) 666.
- 15 Rukmanikrishnan B, Ismail F R M, Manoharan R K, Kim S S & Lee J, Blends of gellan gum/xanthan gum/zinc oxide based nanocomposites for packaging application, *Int J Biol Macromol*, 148 (2020) 1182.
- 16 Xie Q, Zheng X, Li L, Ma L, Zhao Q, Chang S & You L, Effect of curcumin addition on the properties of biodegradable pectin/chitosan films, *Molecules*, 26 (2021) 2152.
- 17 Xu Y X, Kim K M, Hanna M A & Nag D, Chitosan-starch composite film: Preparation and characterization, *Ind Crops Prod*, 21 (2005) 185.
- 18 Raghunath A & Pereira E, Antioxidant effects of quercetin, vitamin C, and ZnO nanoparticles on streptozotocin-induced diabetic rats, *Colloids Surf B: Biointerf*, 151 (2017) 120.
- 19 Bhuyan T, Misra K & Dhiman M, Synthesis of ZnO nanoparticles by two different methods and study of their structural, optical, morphological and photocatalytic properties, *Appl Surf Sci*, 345 (2015) 29.
- 20 Pawade V B, Lanje V H, Ghate P D, Janbandhu K S & Lakhawat G P, IR reflective performance of ZnO: Dy pigment on glass surface, *Mater Lett*, 374 (2024) 137121.
- 21 Chanpurkar R S, Lakhawat G P & Khonde R D, Synthesis, analysis, and application of lactide-based polyester as coating with improved mechanical and rheological behavior, *J Coat Technol Res*, 18 (2021) 1659.